Engineering and Technology Journal
Journal homepage: https://etj.uotechnology.edu.iq

The Effect of Ceo_2 Addition on Transformation Temperatures and Wear Resistance of Cu-Al-Ni Shape Memory Alloys

Dina F. Hammadi*, Raad S. Ahmed Adnan, Mohammed A. Al-Sarraf

Materials Engineering Dept., University of Technology-Iraq, Alsina'a street, 10066 Baghdad, Iraq.
*Corresponding author Email: mailto:mae.19.26@grad.uotechnology.edu.iq.

HIGHLIGHTS

- Enhance Transformations Temperature for SMAs by adding CeO_2 particles with different percentages.
- Enhance Wear behavior for SMAs BY adding CeO_2 particles with different percentages.
- Enhance Hardness for SMAs BY adding CeO_2 particles with different percentages.

ARTICLE INFO

Handling editor: Akram R. Jabur

Keywords:
Shape Memory Alloys; Wear behavior; Ceramics; DSC; Transformation Temperature.

ABSTRACT

SMAs can switch from one crystallographic structure to another in response to temperature or stress stimuli. When SMAs are exposed to mechanical cyclic stress, they can absorb and discharge mechanical energy by experiencing a reversible hysteretic shape change. SMAs are widely used for sensing, actuation, impact absorption, and vibration damping. This work studied the effect of CeO_2 addition on the transformation temperature and wear resistance of Cu-Al-Ni SMAs. WhereCeO_2 was added at different percent's 0.5, 1, and 3 wt% to the base alloy, followed by casting and homogenization at 900ºC. Some tests were carried out: Differential scanning calorimeter, Optical Microscope, Scanning Electron microscopy, Energy dispersion spectrometer, X-Ray Diffraction, and Wear and Hardness tests. OM and SEM tests reveal that both phases of martensite β and γ are found. Also, the additions of CeO_2 show a visible effect on phase formation and transformation temperatures. It was observed that increasing of CeO2 particles in Cu-based SMAs owing to improve interfacial bonding between matrix and reinforcement and also observed that the variants become thicker with increasing in percent. Additions of different percentages of cerium oxide increase the hardness of Cu-Al-Ni SMAs. Due to the addition of CeO_2 particles, the sample's wear rate decreases compared to pure SMAs.

1. Introduction

The shape memory alloys (SMAs) can remember and restore their previous shape after substantial inelastic deformation through a phase transformation mechanism. The shape memory effect is the name for SMA's unique characteristic (SME). SMA phase change may be induced by either sending an electrical current through the structure or increasing the structure's temperature over its phase transformation temperature with an external heat source [1]. Cu-based SMAs are in high demand because of their low cost and excellent mechanical and shape memory capabilities. In various applications, copper-based alloys are an excellent replacement for Ni-Ti alloys, such as micro-electro-mechanical systems, valves, actuators, and dampers, since they are inexpensive and easy to manufacture and have a wide temperature range [2]**.** Cu-based alloys with the characteristics of high tensile strength and hardness require extensive research and development. Age hardening or adding dispersed particles to copper's matrix can significantly improve its mechanical strength. At high temperatures, age-hardenable copper alloys are prone to precipitate coarsening, significantly reducing their strength. This way, even when exposed to high temperatures, dispersion-strengthened copper preserves most of its properties. Insoluble in the copper matrix, dispersed particles including oxides, carbides, and borides are thermally stable at high temperatures. Dispersion-strengthened copper alloys that have been dispersion-strengthened are used to make copper-based matrix composites [3-6]. Wang et al. [7] had shown some oxides can exhibit exceptional shape memory effects and superelasticity at nano/microscales, as evidenced by recent development in shape memory oxide studies connected to small-scale approaches such as lowering grain boundaries, strain engineering, and use in the form of nanoscale thin films. The shape memory efficiency of the materials systems ZrO_2, $BiFO_3$, and VO_2 in bulk and small-scale is reviewed. Pandey et al. [8] investigated the effect of adding nano CeO2 to a well-known Cu-Al-Ni shape memory alloy as a grain pinner/refiner. They discovered a very uniform dispersion of CeO_2 and that increasing CeO_2 resulted in a superior martensitic structure. The inclusion of CeO_2 substantially impacts transition temperature and phase formation. In addition,

http://doi.org/10.30684/etj.2022.132840.1144
Received 21 January 2022; Accepted 25 July 2022; Available online 23 September 2022
2412-0758/University of Technology-Iraq, Baghdad, Iraq

Pandey et al. [9] studied the addition of nano-CeO_2 and modified the morphologies of microstructures significantly. 0.1% CeO_2 addition was reported to have the highest mechanical (fracture stress=536 MPa and fracture strain=7.67%) and shape memory properties (95% shape recovery). The addition beyond this was detrimental to mechanical and shape memory properties. In one of the studies, Abolhasani et al. [10] reported employing a new way to boost the shape memory effect and its stability in Cu-Al-Ni SMAs by selective laser melting and partial reinforcement with alumina (Al_2O_3). Partially reinforced sections with 0.3 wt% and 0.9 wt% Al_2O_3 are compared to fully reinforced parts to define the effect of partial reinforcement. The shape memory effect is improved by enhancing mechanical anisotropy in the building direction, resulting in the buildup of localized residual compressive stresses above the reinforcing lines in the neutral plane, generated during selective laser melting. Furthermore, a unique phenomenon known as the "waistband effect" is seen in cyclic compressive operation, which results in incremental penetration of the reinforcing particles into the neutral plane during compression. These findings show that partial reinforcement with Al_2O_3 improves the shape memory effect of Cu-Al-Ni SMAs substantially. Xie Dong et al,[11] studied TiO_2 coatings with thicknesses of 100 and 50 nm on NiTi shape memory alloys were created using high-power impulse magnetron sputtering (SMA-NiTi). Under uniaxial strain, the NiTi substrate transitioned from B_2 to B_{19}' martensitic phase. Surface relief appeared on the film after stress relaxation, but residual deformation in the NiTi persisted. After heating, a reverse B_{19}' to B_2 martensitic phase transition occurred on a Ni-Ti substrate, removing surface relief and residual deformation. The 50-nm film showed no breaking or spalling after tensile deformation at a maximum strain of10%, and the shape was recovered by heating. In a similar line, the current work investigates the microstructure, hardness, phase precipitation, and transition temperature of-14 wt pct Al-4.5 wt pct Ni when various quantities of (CeO_2) Micro particles are introduced to CuAlNi SMAs. CuAlNi SMA was studied using X-ray diffraction (XRD), differential scanning calorimetry (DSC), scanning electron microscopy (SEM), optical microscopy (OM), as well as hardness and wear testing.

2. Experimental Study

2.1 Preparation of the Sample

Three alloys with varying CeO_2 compositions were created in a gas furnace at 1400°C with a protective environment of (Ar) Gas, as shown in Table1. To make the ingots, pure metals such as Cu (99.99 percent), Al (99.999 percent), Ni (99.9 percent), and CeO_2 (99.95 percent) were wrapped in Al foils and placed in a silicon carbide crucible. The produced ingots are cylindrical, with a diameter of 14 mm and a height of 117 mm. Homogenization was performed on all ingots in a Carbolite1500, England furnace at 1173 K (900 ^{0}C) for 30 minutes, followed by iced water quenching. A wire cut device EDM was also used to divide the samples into two groups of specimens. For microstructure testing, the first one has a 14mm diameter and a 5mm length. For the wear test, the second was machined by wire cutting to 14mm diameter and 30mm height.

Table 1: Specimen coding and composition of the materials

Sample Composition	Sample Code
Cu-14wt pctAl-4.5wt pct Ni	C
Cu-14wt %Al-4.5wt%Ni +0.5 wt % CeO_2	C1
Cu-14wt %Al-4.5wt%Ni +1 wt % CeO_2	C2
Cu-14wt %Al-4.5wt%Ni +3 wt % CeO_2	C3

2.2 Xrd and Microstructure Tests

X-Ray Diffraction testing was used to detect the phases and compounds that precipitated in all of the alloys generated. The inspections were carried out with (ASCII-2Theta-Intensity (ASC)), (K-1=1.54060), and the supplied voltage and current were 40 KV and 30 mA, respectively. In addition, SEM was also utilized to evaluate the surface morphology and microstructure of the samples (SEM Tescan Mira3 XMU, Czech Republic).

2.3 Dsc Test

Differential scanning calorimetry is commonly used to examine the thermal properties of SMAs. A mechanical saw was used to cut the specimen, which was then placed in a tiny crucible weighing 100mg and heated for 10 minutes at 400°C. The DSC was carried out in the Materials Engineering department DSC using (DSC131EVO-SETARAM DSC Device). Also, the equilibrium temperature is calculated from Equation 1. According to Salzbrenner and Cohen, the equilibrium temperature is characterized by the following relationship [12]:

$$T^0 = 0.5\,(M_s + A_f) \quad (1)$$

$$\text{Hysteresis} = A_s - M_f \quad (2)$$

$$\text{Spread} = A_f - A_s \quad (3)$$

The martensite starts temperature is M_s, while the austenite finishing temperature is A_f. During heating and cooling cycles, the endothermic and exothermic peaks acquired from DSC data were combined as a function of temperature. Hysteresis from Equation 2 [13], and spread from Equation 3 [13].

2.4 Hardness and Wear Tests

All samples were subjected to a Vickers micro-hardness test using an HVS100 Microhardness tester with a force of 2.94N and a holding duration of 15 seconds. Because there may have been holes on the sample's surface that would alter the hardness assessment, two readings were collected for each sample. In the wear test, pin-on-disc equipment was utilized to examine the wear attributes of the composite. Each composite sample was put through a wear test with a continuous load of 15 N at a constant speed of 1 m/s for 5, 10, and 15 minutes at a constant sliding distance of 62.5 m using 180 mesh Al_2O_3 paper. The wear pin was cleaned in acetone and dried before being weighed on a micro-balance with a 0.1 mg sensitivity before wear testing. Adhesive wear equations are given by the following expressions:

$$V = K\,WL\,/H_V \qquad (4)$$

W represents weight, L is the sliding distance, and K stands for wear coefficient, which is determined by the plasticity index, surface roughness, and friction coefficient [14].

3. Results and Discussion

A composite reinforcement's content and size are directly related to its microstructure and mechanical characteristics.

3.1 Dsc Test

Cerium dioxide additions for the three alloys produce well-defined peaks once more. The CeO_2+Base SMA transition temperature and equilibrium temperature findings are shown in Table 2. The kind and shape of the martensite phase and the order and stability at a degree of γ ' have a role in the transition temperature fluctuation. The forward (cooling) and reverse (heating) martensitic transformations are confirmed by the peaks in Figures 1(A, B, C, and D). The transformation went to a higher temperature for each sample for the three alloys. Thermal cycling up to 200°C is well recognized for causing changes in alloy structure and composition and physical and mechanical characteristics[15]. After a suitably long aging period at 200°C, an increase in the critical transition temperatures associated with a conversion of γ ' into $\beta`_1$ martensite was also identified. [16]. The DSC thermograms for the base alloy show transformation temperature in the domain between(-100-1700C), also shown in [17]. In terms of equilibrium temperature, the greatest value of T° was recorded at C_3 alloy with a 3 percent addition, which is connected to martensite phase precipitation and shape. Adding 3% CeO_2 to Mf boosts Mf to 171, according to Table 2. This is because of the quick decline in transformation temperature as grain size increases with CeO_2 concentration.

Table 2: Transition temperature for SMA + CeO_2 alloys

Alloy	As °C	Af °C	Ms°C	Mf°C	T°C	H°C	S°C
C	130	165	125	104	145	26	35
C_1	376	384	166	101	275	274	8
C_2	285	356	172	141	264	144	70
C_3	356	394	210	171	302	184	38

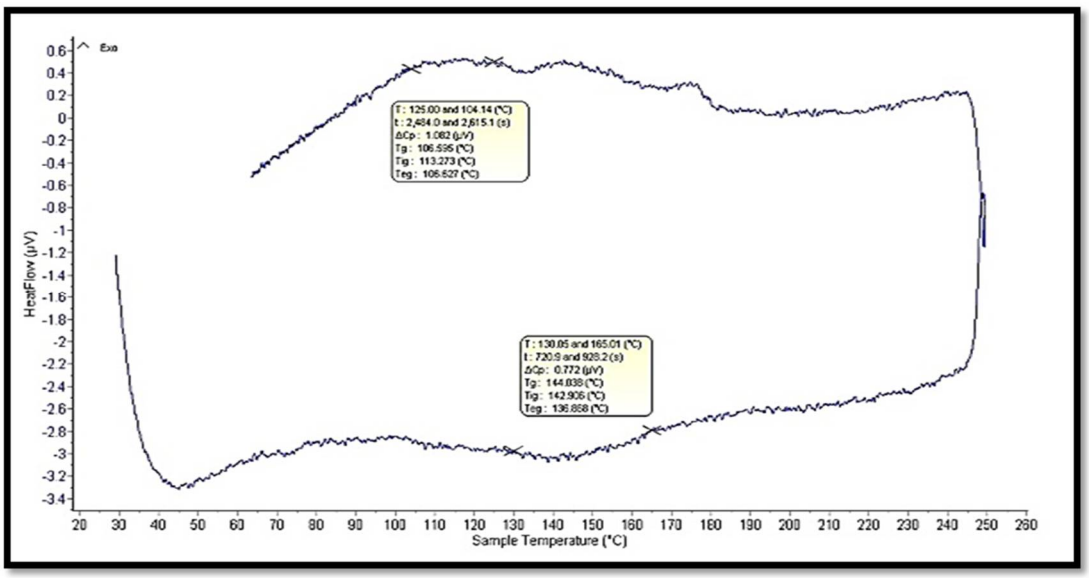

(A)

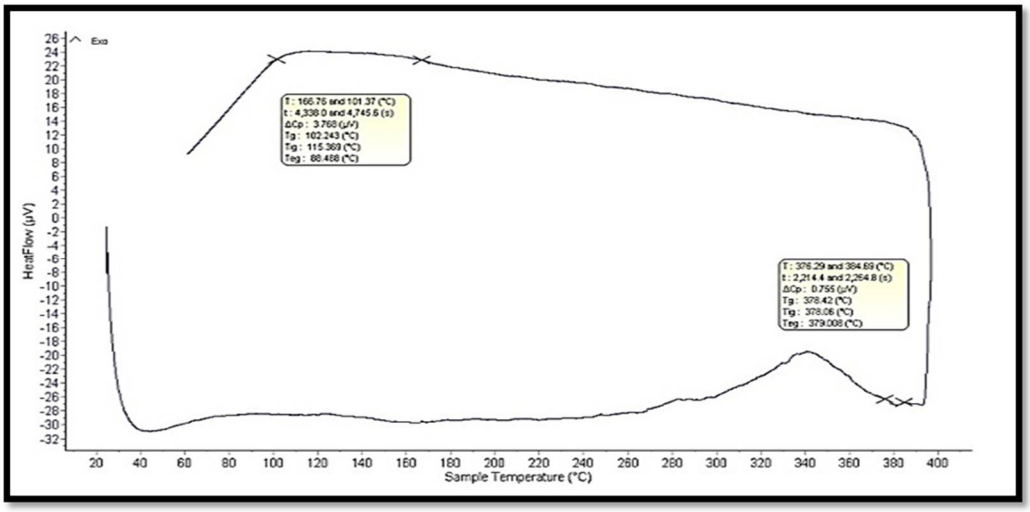

(B)

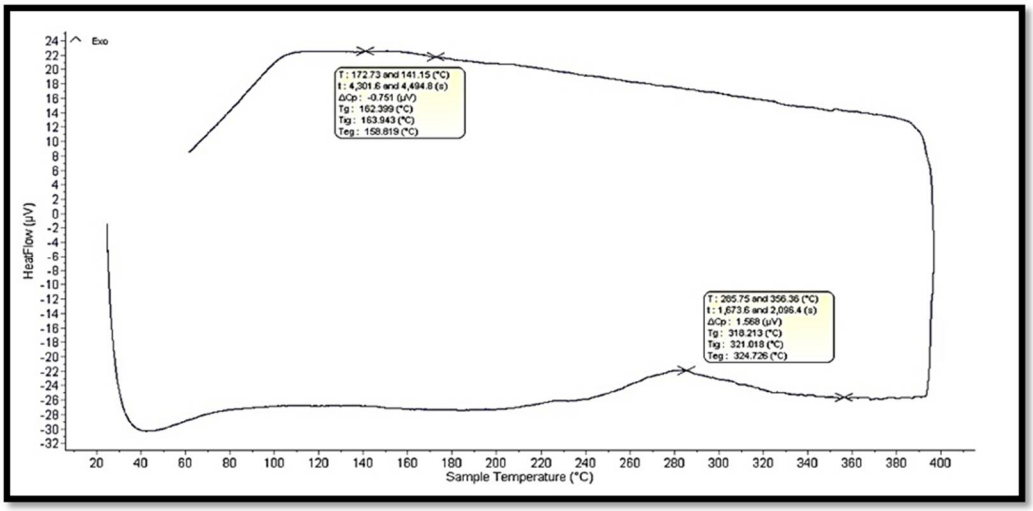

(C)

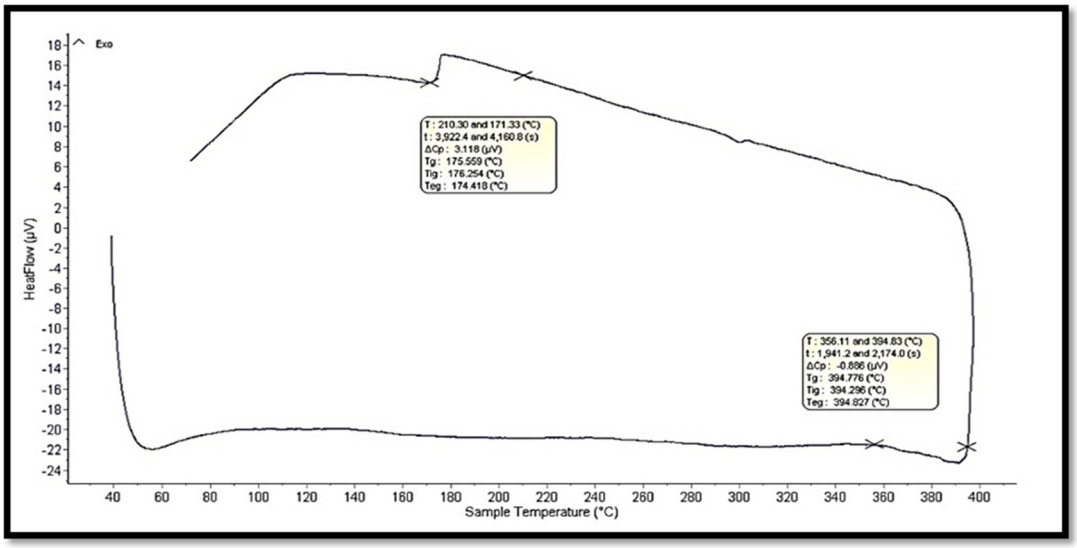

(D)

Figure 1: Displayed DSC Test for A. base alloy B. addition of 0.5 CeO_2 to the base alloy C . addition of 1% CeO_2 to the base D .addition of 3% CeO_2 to the base

3.2 X-Ray Diffraction (XRD) Analysis

Figure 2 A shows the XRD spectrum of Cu-Al-Ni materials with ratios Al (14%), Ni 4.5%, and Cu's rest ratio. The diffraction peaks correspond to the polycrystalline structure. The spectrum curve showed sharp and very fine peaks indicating good structure crystallization. The based alloy SMA for (Cu-Al-Ni) observed that the formation of both phases indicates the form of the both martensitic Cu-Al (β`) at angles (42º, 44º, and 64º) and Cu-Al-Ni (γ`) at angles (24º, 46º, and 74º) respectively. Figure (2) B illustrate the XRD charts for the SMA (Cu-Al-Ni) modified with 0.5% $CeO_2$is found at angles (22º, 31º, and 51º). Also, the (β`) phase Cu-Al (41º, 43º, and 61º) and Cu-Al-Ni (γ`) are found at angles (25º and 75º) phase indices. Figure C illustrates the XRD charts for the SMA (Cu-Al-Ni) modified with 1% CeO_2 found at angles (31º, 39º, 49º, and 51º). Also, the (β`) phase Cu-Al (42º, 44º, and 64º) and Cu-Al-Ni (γ`) are found at angles (27º and 77º) phases, respectively. Finally, D showed the XRD show charts for the SMA (Cu-Al-Ni) modified with 3% CeO_2 found at angles (51º). Also, the (β`) phase Cu-Al (41º and 43º) and Cu-Al-Ni (γ`) are found at angles (25º) phases.

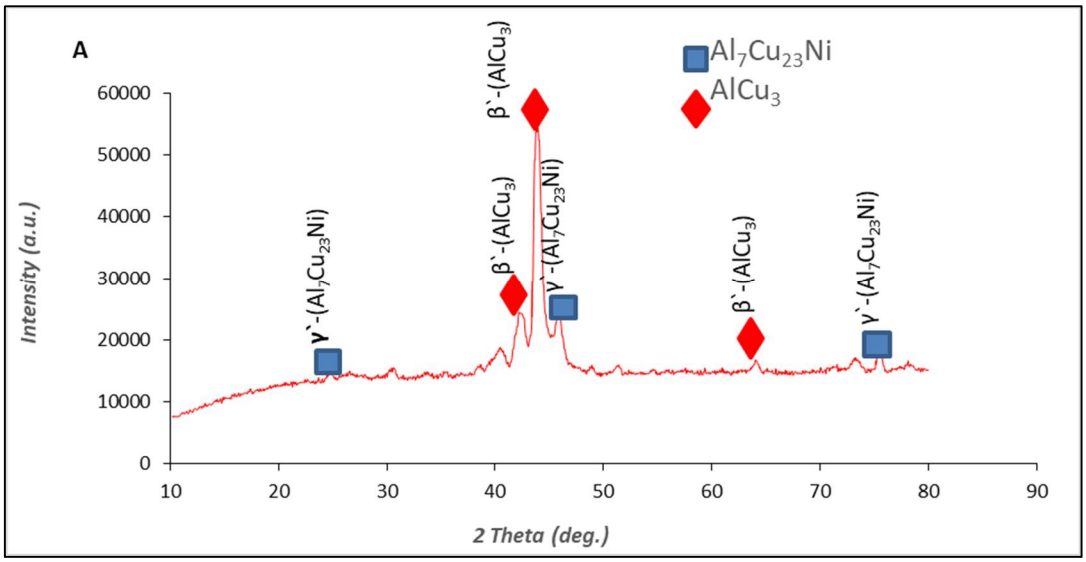

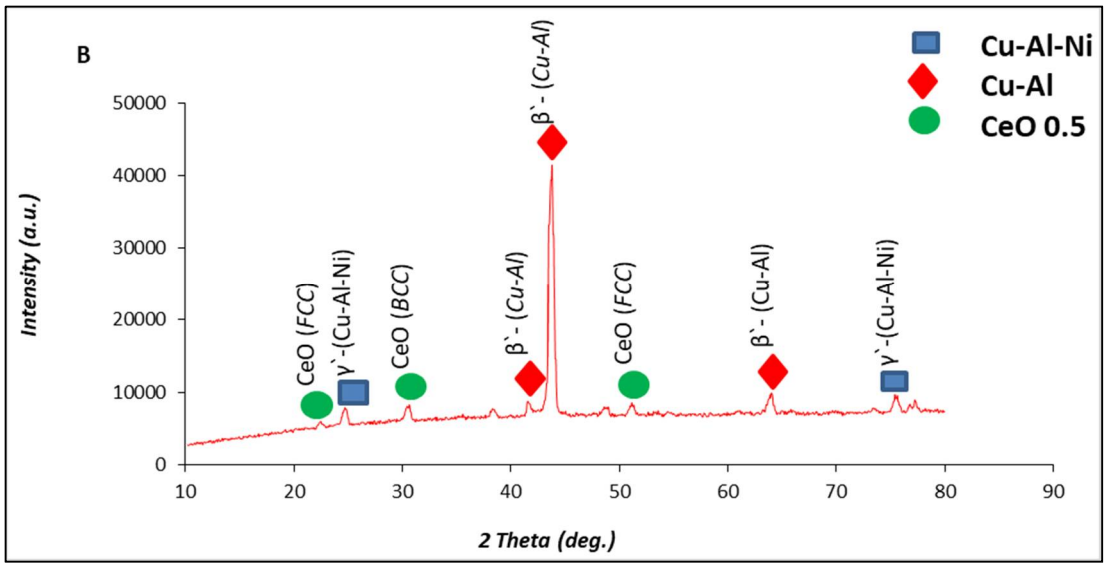

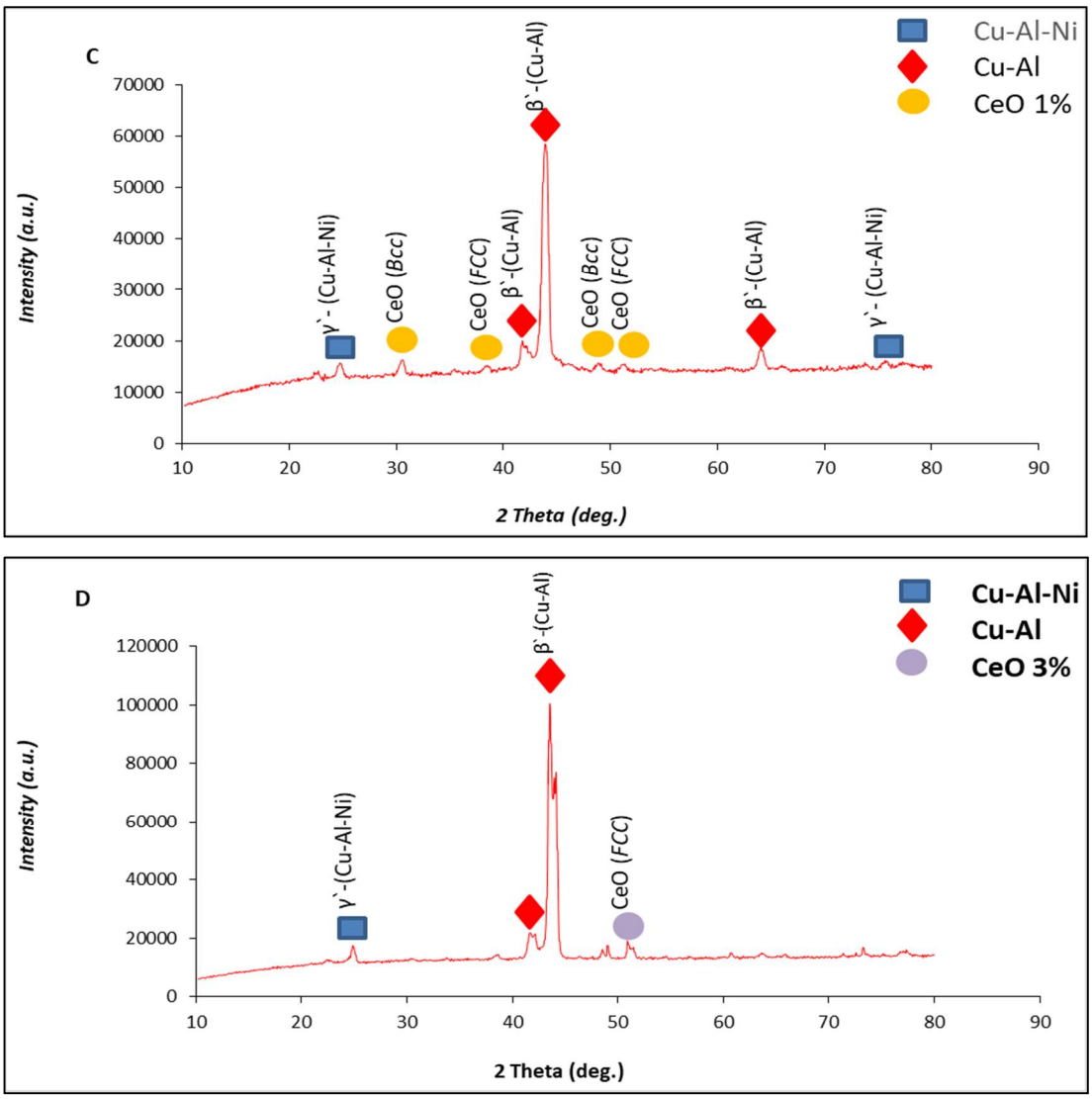

Figure 2: Displayed XRD Test for A .base alloy B. addition of 0.5 CeO_2 to the base alloy C. addition of 1% CeO_2 to the base D .addition of 3% CeO_2 to the base

3.3 Microstructure

The morphology of both martensitic Cu-Al(β`) and Cu-Al-Ni(γ ') is shown in Fig.3.A. These phases are $\beta$`and γ`, which are thermally generated martensites with different thicknesses and orientations. Between the $\gamma$` phases, the γ` phase developed as a plate-like phase, while the $\beta$` phase formed as a needle-like phase. Figure 3B shows the morphology of martensite for the SMA (Cu-Al-Ni) modified with 0.5 percent CeO_2 discovered in the inhomogeneous distribution in the matrix, which gave both phases a fine grain size. Both phases suggest the form of both martensitic Cu-Al(β ') and Cu-Al-Ni (γ '). Figure3.C and D also showed the morphology of martensitic phases β and γ. Also, in the figures b, c, and d displed as the reinforcing content increased from 0.5 to 3%, it was discovered that martensite variations differed in size and thickness. The variants become thicker, as observed at Abohasani[9] when they added alumina to CuAlNi SMAs. Figures 4 B, C, and D showed SEM images, which also confirm [9] and reveal that the increase of CeO_2 content increases the hardness of the samples. Figure 5 A, B, C, and D showed the EDS test for all the samples and the content of the elements.

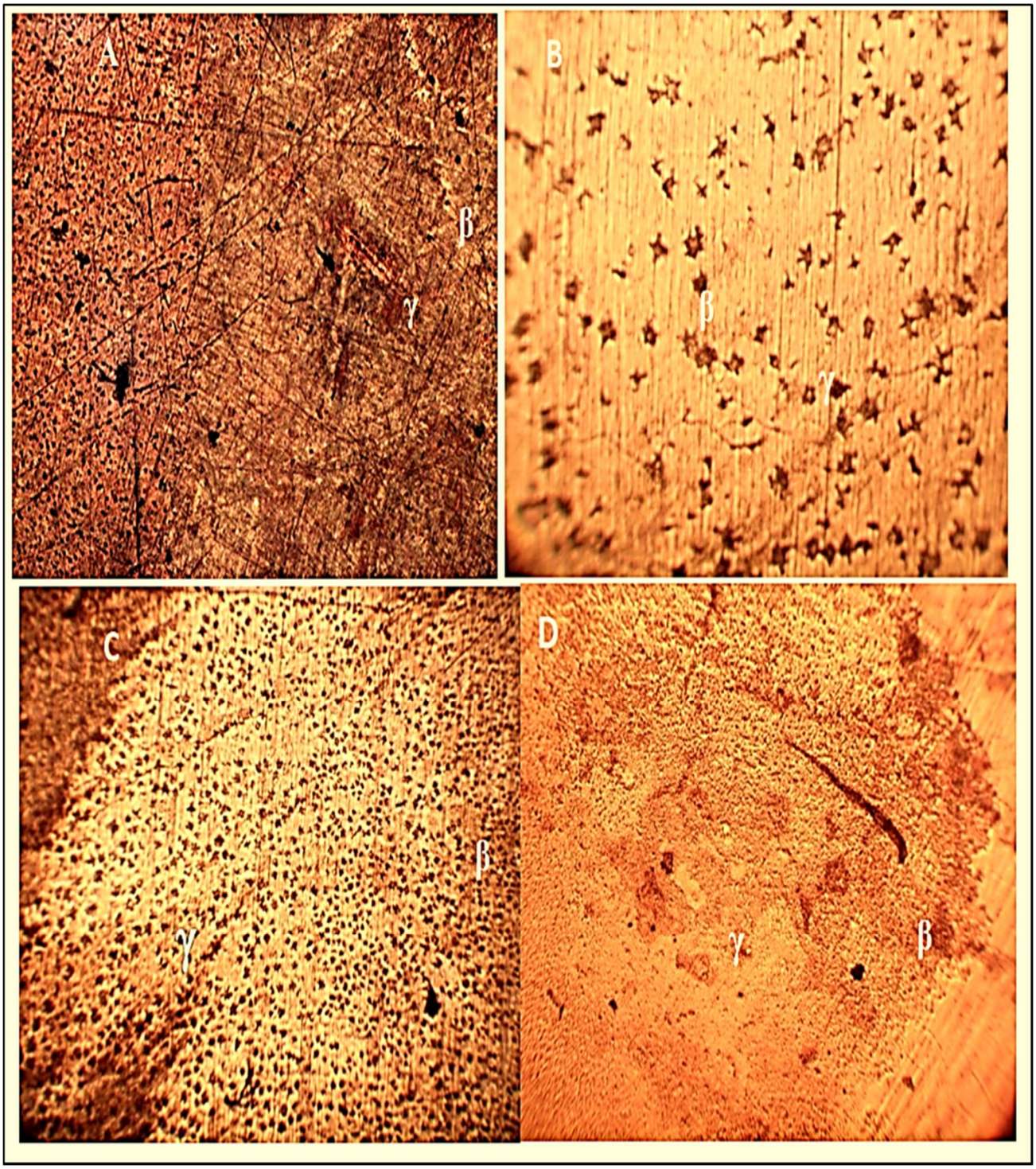

Figure 3: Displayed OM Test for A. base alloy B. addition of 0.5 CeO_2 to the base alloy C. addition of 1% CeO_2 to the base D. addition of 3% CeO_2 to the base

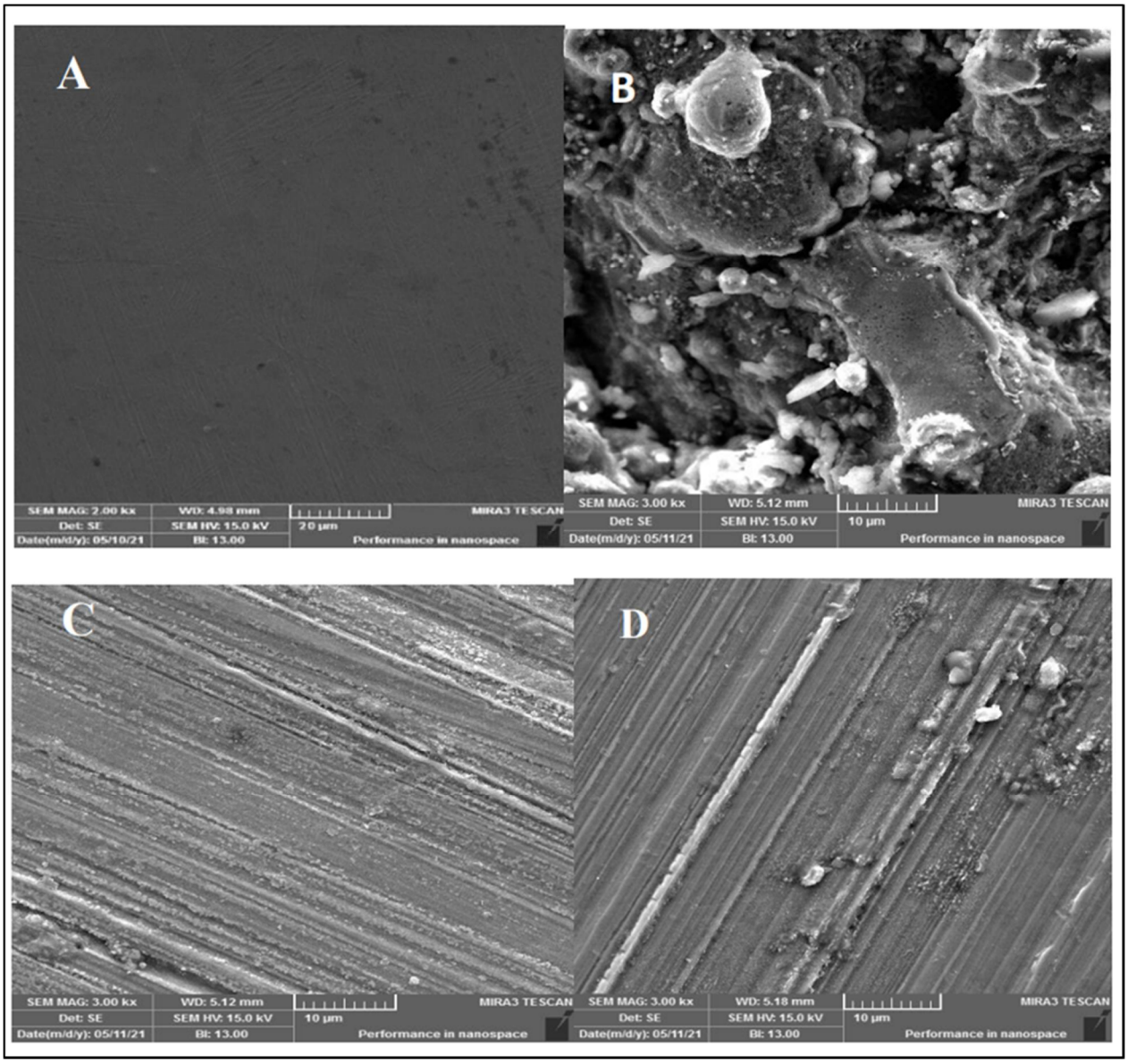

Figure 4: Displayed SEM test for A.base alloy B. addition of 0.5 CeO_2 to the base alloy C. addition of 1% CeO_2 to the base D .addition of 3% CeO_2 to the base

3.4 Hardness and Wear Test

The average of two measurements was used to calculate microhardness, as shown in Figure 6. The hardness rose by adding 0.5 percent, with a measurement of 475.9Hv compared to the basic SMA. However, with additional addition, the hardness decreased, as shown in the table, at a percentage of 1% weight percent CeO_2. The hardness was also observed to increase when adding 3% weight percent CeO2. This is a little difference in hardness in certain cases, which may be attributable to the presence of various phases in the samples. This confirms what we discovered in [8]. The wear rates of the composite were lower than those of pure Cu-Al-Ni at different periods, as indicated in Figure7. An increase in wear volume with increasing time at constant load may be seen in the graph. When CeO_2 0.5 weight percent is added to the base SMAs, the wear rate of the sample decreases compared to pure base SMA. This is due to the integration of CeO_2 particles, which increases the hardness of the specimen. Also, observe that the weight loss for adding 0.5 weight percent, 3 weight percent CeO_2 is slightly different from the previous additions.

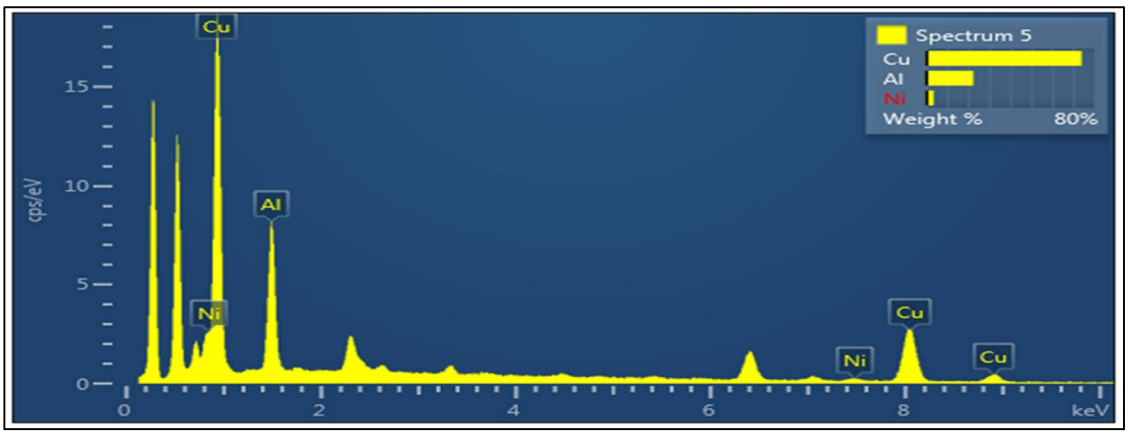

(A)

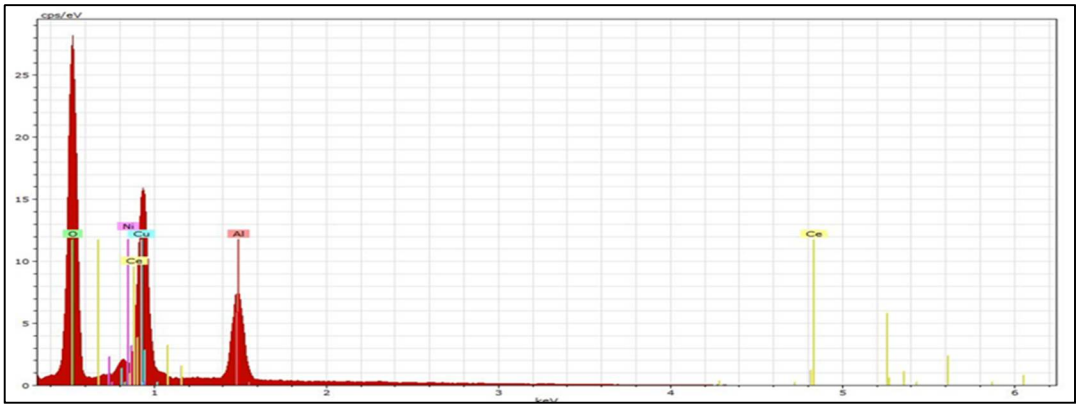

(B)

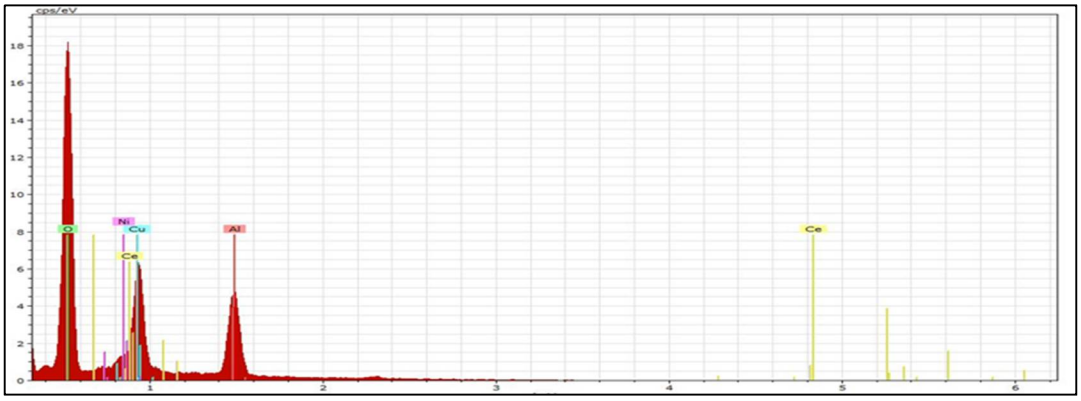

(C)

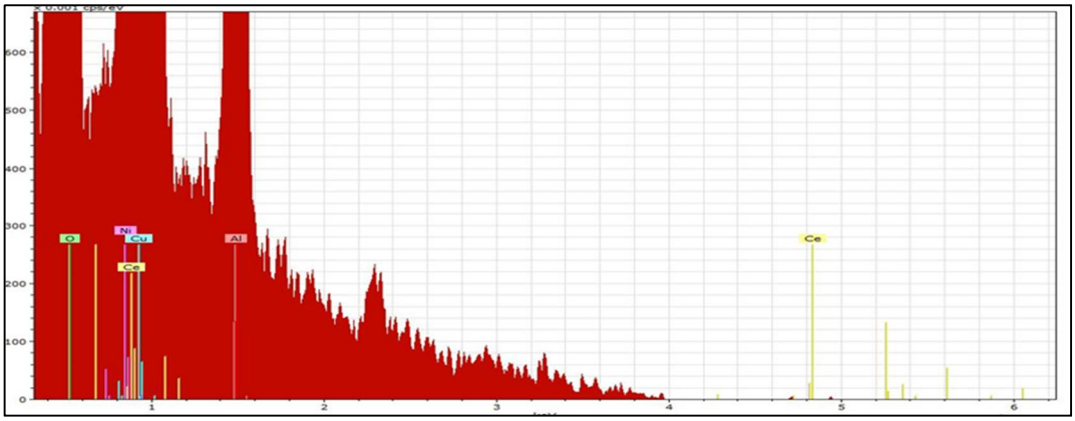

(D)

Figure 5: Displayed EDS Test for A .base alloy B. C_1, C . C_2, D C_3

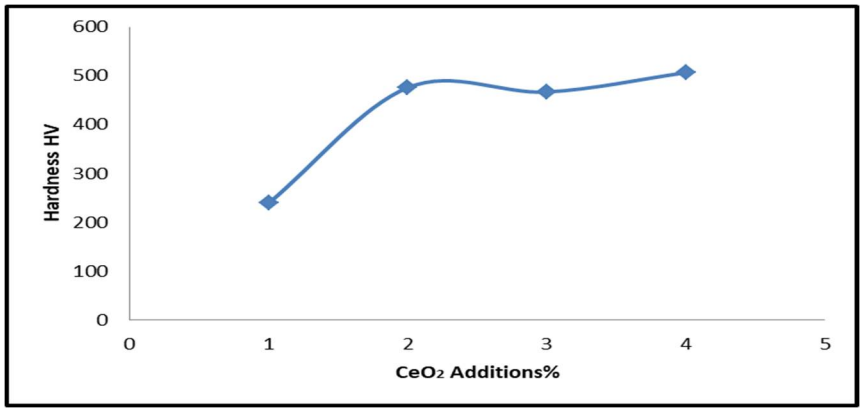

Figure 6: Variation of Hardness with different CeO_2 additions

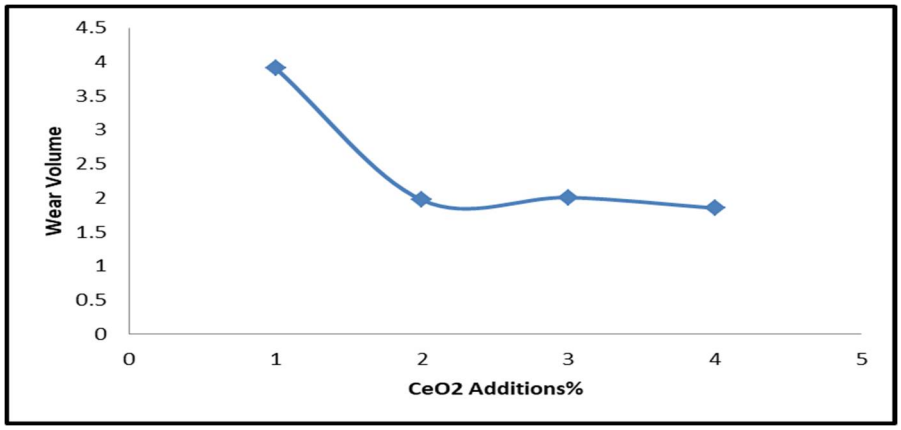

Figure 7: Variation of wear Volume rate with different CeO_2 additions

4. Conclusion

This article examined the effect of adding CeO_2. The following conclusions can be taken from the report results:

1) From transition temperature for SMA modified with CeO_2 addition, there is an increase in Ms and Mf and hysteresis and spread. Also, the greatest value of T^0 was found in the C_3 alloy, which is attributed to martensite phase precipitation and shape.
2) From SEM and OM images, both phases denote the martensitic Cu-Al (β`) and Cu-Al-Ni(γ`) phases, respectively. These phases are β` and γ`, produced as thermally induced martensites with varying thicknesses and orientations. It was observed that increasing CeO_2 particles in bronze matrix owing to improved interfacial bonding between matrix and reinforcement and that the variants become thicker with increasing in percent.
3) From the hardness test, we can see that the additions of different percent of cerium oxide increase the hardness of Cu-Al-Ni SMAs, Where the highest hardness was in sample C_3. Furthermore, from the wear test, we can see that when CeO2 was 0.5 added to the base SMA, the wear rate of the sample decreased compared to pure SMA. This is due to the addition of CeO_2 particles, which decrease the wear rate of the specimen.

Acknowledgments

The authors would like to express their appreciation to the Resistance Laboratory at the University of Technology in Baghdad, Iraq, for their support in conducting the wear test. The Calorimetric Differential Scan Test was conducted with the help of the employees of the Materials Testing Laboratory at the Materials Engineering Department at the University of Technology in Baghdad, Iraq.

Author contribution

All authors contributed equally to this work.

Funding

This research received no specific grant from any funding agency in the public, commercial, or not-for-profit sectors.

Data availability statement

The data that support the findings of this study are available on request from the corresponding author.

Conflicts of interest

The authors declare that there is no conflict of interest.

References

[1] C. Yang, S. Abanteriba, A. Becker, A review of shape memory alloy based filtration devices, AIP Adv., 10 (2020) 060701. https://doi.org/10.1063/1.5133981

[2] J. Van Humbeeck, Non-medical applications of shape memory alloys, Mater. Sci. Eng. A, 273-275 (1999) 134–148. https://doi.org/10.1016/s0921-5093(99)00293-2

[3] A. Upadhyaya, Sintering of copper-alumina composites through blending and mechanical alloying powder metallurgy routes, Mater. Des., 16 (1996) 41–45. https://doi.org/10.1016/0261-3069(95)00006-K

[4] JS. E. Broyles, K. R. Anderson, J. R. Groza, J. C. Gibeling, Creep deformation of dispersion- stregthened copper, Metall .Mater. Trans. A, 27 (1996)1217–1227. https://doi.org/10.1007/BF02649859

[5] Y.L Wang , Y.Z Wan, X.H Dong , G.X Cheng , H.M Tao , T.Y Wen, preparation and characterization of antibacterial viscose-based activated carbon fiber supporting silver, Carbon, 36 (1998) 1567–1571. https://doi.org/10.1016/s0008-6223(98)00101-8

[6] S. A. J. Lee, N.J. Kim, J.Y. Jung, E.S. Lee, Preparation and characterization of antibacterial viscose-based activated carbon fiber supporting silver. , Scr. Mater, 1063–69.

[7] X. Wang and A. Ludwig, Recent Developments in Small-Scale Shape Memory Oxides, Shape Mem. Superelasticity.6 (2020) 287–300. https://doi.org/10.1007/s40830-020-00299-7

[8] A. Pandey, A. K. Jain, S. Hussain, V. Sampath, and R. Dasgupta, Effect of Nano CeO2 Addition on the Microstructure and Properties of a Cu-Al-Ni Shape Memory Alloy, Metall. Mater. Trans. B Process Metall. Mater. Process. Sci., 47 (2016) 2205–2210. https://doi.org/10.1007/s11663-016-0691-0

[9] S. Hussain, A. Pandey, and R. Dasgupta, Nano □ CeO 2 Doped Cu – Al – Ni SMAs with Enhanced Mechanical as well as Shape Recovery Characteristics, Met. Mater. Int., (2019)1–5. https://doi.org/10.1007/s12540-019-00570-2

[10] D. Abolhasani, S. W. Han, C. J. VanTyne, N. Kang, and Y. H. Moon, Enhancing the shape memory effect of Cu-Al-Ni alloys via partial reinforcement by alumina through selective laser melting, J. Mater. Res. Technol., 2021. https://doi.org/10.1016/j.jmrt.2021.10.040

[11] X. Dong, Y. Fei, J.B. Wang, Y.Y. Su, F.J. Jing, Y.X. Leng, Nan Huang, Deformation behavior of TiO2 films deposited on NiTi shape memory alloy after tensile and water-bath heating tests, Surf. Coatings Technol., 416 (2021). https://doi.org/10.1016/j.surfcoat.2021.127151

[12] R. J. Salzbrenner, M. Cohen , On the thermodynamics of thermoelastic martensitic transformations. Acta Metall. 27 (1979) 739–748. https://doi.org/10.1016/0001-6160(79)90107-X

[13] Lexcellent. Christian Shape Memory Alloy Handbook john wiley and son , NewYork,USA, dition, 2013.

[14] Kato, K. and Hokkirigawa, K., Abrasive Wear Diagram, in Proceedings of Eurotrib', Elsevier, Amsterdam, 1985.

[15] L. A. Matlakhova, E. C. Pereira, S. A. Pulnev, C. Y. Shigue, N.A. Palii, Physical and Structural Characterization of Monocrystalline Cu-13.7% Al-4.2% Ni Alloy Submitted to Thermo-Cyclical Treatments under Applied Loads, Metals, 10 (2020) 219. https://doi.org/doi:10.3390/met10020219

[16] V. E. A. Araujo, R. Gastien , E. , Zelaya J. I. Beiroa ,Corro I, Sade M, et al. Effects on the martensitic transformations and the microstructure of CuAlNi single crystals after ageing at 473 K, J. Alloys Compd., 641 (2015) 155-161. https://doi.org/10.1016/j.jallcom.2015.04.065

[17] R. Suhail, A. Adnan, M. K. Abbass, M. M. Al-Kubaisy, R. S. A. Adnan, The effect of thermo-mechanical treatment on mechanical properties & microstructure for (Cu-Al-Ni) shape memory alloy, Eng. Technol. J., 34 (2016) 2518–2526. https://doi.org/10.30684/etj.34.13A.14